Switching friction at a manganite surface using electric fields

H. Schmidt,[1] J.-O. Krisponeit [2,3] N. Weber [1] K. Samwer [2,4] and C. A. Volkert [1,4,*]

[1]*Institute of Materials Physics, University of Göttingen, 37077 Göttingen, Germany*
[2]*1st Physics Institute, University of Göttingen, 37077 Göttingen, Germany*
[3]*Institute of Solid State Physics, University of Bremen, 28359 Bremen, Germany*
[4]*The International Center for Advanced Studies of Energy Conversion (ICASEC), University of Göttingen, 37077 Göttingen, Germany*

We report active control of the friction force at the contact between a nanoscale asperity and a $La_{0.55}Ca_{0.45}MnO_3$ (LCMO) thin film using electric fields. We use friction force microscopy under ultrahigh vacuum conditions to measure the friction force as we change the film resistive state by electric-field-induced resistive switching. Friction forces are high in the insulating state and clearly change to lower values when the probed local region is switched to the conducting state. Upon switching back to an insulating state, the friction forces increase again. Thus we demonstrate active control of friction without having to change the contact temperature or pressure. By comparing with measurements of friction at the metal-to-insulator transition and with the effect of applied voltage on adhesion, we rule out electronic excitations, electrostatic forces, and changes in contact area as the reasons for the effect of resistive switching on friction. Instead, we argue that friction is limited by phonon relaxation times, which are strongly coupled to the electronic degrees of freedom through distortions of the MnO_6 octahedra. The concept of controlling friction forces by electric fields should be applicable to any materials where the field produces strong changes in phonon lifetimes.

I. INTRODUCTION

Friction is a complex phenomenon that occurs between two bodies at a sliding contact. Despite the fact that it often can be described by straightforward empirical relations, its fundamental cause is by no means simple. With the advent of the atomic force microscope (AFM), understanding and controlling nanoscale friction has become one of the major interests in modern tribology. A promising direction is reported in several literature studies [1–9] which show a clear change in measured nanoscale friction force when the electronic state of the material is altered. Abrupt increases are observed in the noncontact dissipation of Nb [5] and the contact friction of YBCO [6] and Pb [1,8] as the materials are heated through their superconducting transitions. Contact friction measurements on Si [4] and GaAs [2] semiconductors demonstrate a strong dependence on the charge carrier density, while the contact friction of VO_2 is strongly increased on heating through the metal-to-insulator transition (MIT) from the insulating to the metallic state [3,7].

Although the literature consistently reveals an impact of the electronic state on friction, a clear understanding of the origin of the effect has not yet emerged. The available theories based on the conversion of mechanical energy into electronic excitations predict only small increases in friction when the number of accessible electronic states are increased, while the experiments often reveal much larger changes in friction. As a result, most studies have explained the effect of changes in the electronic state on friction through electrostatic interactions. Coulomb and capacitive forces at the surfaces of dielectrics (including at surface oxides on conductors) can easily be large enough to explain the observed changes in friction [2–4,6,10]. But even in the absence of a full explanation, the pervasiveness of the effect of electronic states on friction raises the intriguing question of whether they can be used to control friction.

Most of the literature studies up until now have used temperature [5,6], contact pressure [3,7], or a sustained bias voltage [2,4,11] between the tip and the sample to control the electronic state of the material. From a practical point of view, it would be advantageous to find a way to control friction without having to change a process parameter such as pressure or temperature or without having to maintain a voltage between the two contact surfaces.

In this study we report on active control of friction by electric-field-induced resistive switching of the surface region of a manganite film. Perovskite manganites offer a range of different electronic state transformations [12], including the well-known temperature-driven metal-to-insulator transition [9,13], the colossal magnetoresistance (CMR) effect [14], as well as bipolar nanoscale resistive switching driven by electric fields [15]. Here we use the last to reversibly alter the resistive state of a nanoscale region of a perovskite manganite surface to investigate the effect on friction using AFM-based methods. In order to get at the origins of the observed changes in friction due to resistive switching, we compare it with the friction behavior observed on heating the film through the metal-to-insulator transition as well as with the effect of applied voltage on the adhesive force.

*Author to whom correspondence should be addressed: volkert@ump.gwdg.de

II. EXPERIMENTAL DETAILS

The manganite $La_{0.55}Ca_{0.45}MnO_3$ thin films were deposited on MgO substrates with (100) orientation by the metalorganic-aerosol deposition technique [16]. Small-angle x-ray scattering gives a film thickness of approximately 44 nm for the film used for the friction measurements, and $\theta/2\theta$ x-ray diffraction experiments confirm (100) epitaxial growth on the substrate and a lattice constant of 3.87(3) Å (see the Supplemental Material [17]). The film sheet resistance vs temperature behavior probed using four-point measurements shows a clear metal-to-insulator transition at $T_{MI} = 245$ K (see the Supplemental Material [17]). The measurements are consistent with the phase diagram for a Ca doping fraction of 0.45, which shows a transition from a ferromagnetic metal to a paramagnetic insulator at 245 K [13]. The films are well known to show reversible resistive switching, with a polarity and behavior depending on the electrode materials [18]; we have also demonstrated that the films can be reversibly switched on the nanoscale by conductive atomic force microscopy (C-AFM) [19,20].

Friction force measurements and resistive switching have been performed in an ultrahigh vacuum chamber with an Omicron VT-AFM/STM at a base pressure of 2×10^{-10} mbar. For the friction experiments we performed friction force microscopy (FFM) using standard platinum-coated Si cantilevers (MikroMasch DPE17/Al BS) as well as standard Si cantilevers (Nanosensors PPP-CONTSCR) with normal spring constants of 0.2 and 0.5 N/m, respectively. The lateral forces were not calibrated [21] but were estimated based on the lateral forces and friction coefficients obtained from a study on a similar manganite film [9]. Thus the values of the friction forces reported here should be understood as order-of-magnitude estimates; nonetheless, relative changes with normal force, switching state, or voltage are accurate to within the displayed error. During the measurements the normal force was kept constant at $F_N = 5$ nN and the scan velocity was set to 2000 nm/s.

The combination of FFM and C-AFM allows us to simultaneously measure the friction force and to switch the resistive state of the manganite back and forth between the metallic (low resistance state LRS) and insulating states (initial state IS, high resistance state HRS) by applying a voltage larger than the switching voltage threshold $|V_C| \approx 3$ V [19]. Additionally, C-AFM gives us the opportunity to resolve the resistive state during friction measurements by recording current maps at voltages below the switching voltage. In order to avoid plastic protrusions that can be generated by Joule heating under application of the large positive switching voltages used for generating the LRS [19], we rapidly scanned the area of interest several times under an applied bias rather than using prolonged voltage pulses at a fixed cantilever position. Using this method, we avoided any noticeable changes in the surface morphology in our experiments, nor was a correlation between rms surface roughness (typically around 1 nm) and friction or current observed.

The use of Pt-coated tips allows simultaneous measurement of friction, topography, and conductivity, as well as the ability to perform resistive switching. However, coated tips deteriorate more quickly than uncoated tips, presumably due

to deformation and wear during measurement. Further, because of differences in tip shape, tip curvature, tip length, and cantilever dimensions, the friction forces measured with one cantilever are not directly comparable to the values measured with another cantilever. As a result, measurement series as a function of switching state, normal force, and voltage had to each be performed with single cantilevers. Results from a given measurement series were only retained if the friction value measured on returning to the initial conditions at the end of the series produced the same value as at the beginning of the series.

In each resistive switching experiment, the friction forces were measured in a 500×500 nm^2 region on the sample surface by performing 600 friction loops, i.e., by recording the lateral forces experienced by the cantilever tip while scanning forward and backward traces over the sample surface. At the same time, the surface topography was recorded from the vertical deflection of the cantilever. The materials resistive state was also probed during the friction loops by recording the current from an applied voltage of 0.1 V, which is well below the threshold needed for switching. First, friction forces, topography, and current maps were obtained from a 500×500 nm^2 region of the specimen in the insulating initial state (IS). Then the near-surface region was switched to the conducting LRS by rapidly and repetitively scanning over the same region with a tip voltage of $+3.5$ V [19,20]. After obtaining friction forces, topography, and current maps from the switched state, the region was switched back to an insulating HRS using a tip voltage of -3.5 V, and friction, topography, and current maps were obtained once again using a voltage of 0.1 V. This experiment was repeated for several different local regions of interest on the specimen. The current maps confirmed a mostly uniform change in resistive state in the switched region (see the Supplemental Material [17]). However, because the current amplifier reached its saturation limit of 50 nA even at a low bias (0.1 V) in the LRS and because the currents in the insulating states (IS and HRS) are below the detection limit of 0.1 nA, we obtained only threshold information about the resistive state. Resistive switching studies and C-AFM measurements were performed on a number of films of the same composition; friction force measurements were performed on a number of regions of only one representative film.

III. RESULTS AND DISCUSSION

Figures 1(a)–1(c) show topography and lateral force maps of the three states (IS, LRS, and HRS) for a representative region on the sample, all obtained using a normal force of $F_N = 5$ nN. Due to some drift between the tip and specimen during the resistive switching procedure, the scanned regions are slightly displaced relative to each other and have been aligned using the topography maps. The common height and force scales for the three sets of maps show clearly that there are no significant changes in topography but that the lateral forces are strongly reduced in the conducting LRS [Fig. 1(b)]. Variations in the lateral forces are observed within each map that are on a similar length scale as the topography [Figs. 1(a)–1(c)].

The dramatic change in friction forces with resistive state is illustrated most clearly by the friction loops. Figure 2 shows
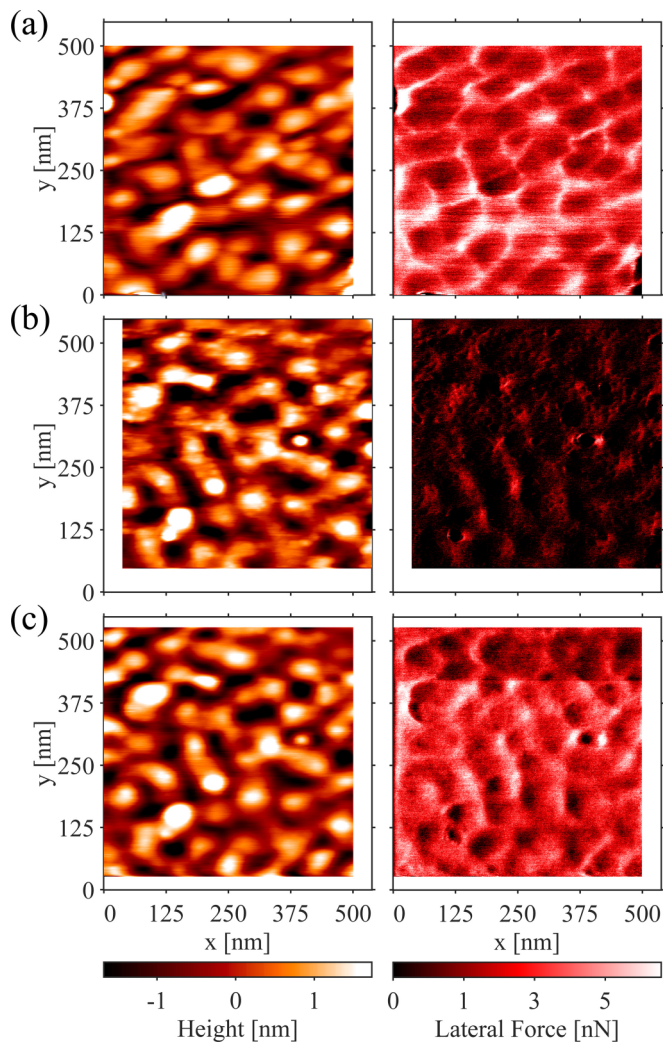
FIG. 1. AFM-based measurements of $La_{0.55}Ca_{0.45}MnO_3$ with a Pt-coated Si tip. (a–c) Topography (left) and lateral force (right) maps obtained from forward traces measured on (a) the initial insulating state (IS), (b) after resistively switching to the metallic state (LRS), and (c) after resistively switching back to the insulating state (HRS).

FIG. 2. Average friction loops for the insulating states (IS = black; HRS = red) and the conducting state (LRS = blue) of $La_{0.55}Ca_{0.45}MnO_3$ obtained with a Pt-coated Si tip. The friction is represented by the difference between the forward (solid line) and backward (dashed line) trace lateral forces divided by 2. Thus the friction is high for the insulating states and low for the conducting state. The slight offset (ca. 15 nm) in the x direction between the forward and backward scans is due to rotation of the tip on reversing the scan direction.

friction loops for each resistive state which have been calculated by averaging the lateral forces for all 600 forward and backward traces within a single region of interest. The exact position of the AFM tip deviates between the forward and backward scan due to torsion of the cantilever and is corrected by determining the maximum correlation between trace and retrace of the topography maps [22]. The x shift of around 50 nm of the LRS loop relative to the IS and HRS has a different origin; it is due to displacement drift that occurred during resistive switching. A clear hysteresis in the lateral force and thus large friction is observed for the initial and switched insulating states (IS and HRS), while the conducting state (LRS) shows almost no hysteresis and thus low friction.

Large variations in lateral force are observed along the forward and backward traces that are correlated with sample position (Fig. 2). These local variations are mostly unchanged on switching to the conducting state and on switching back to the insulating st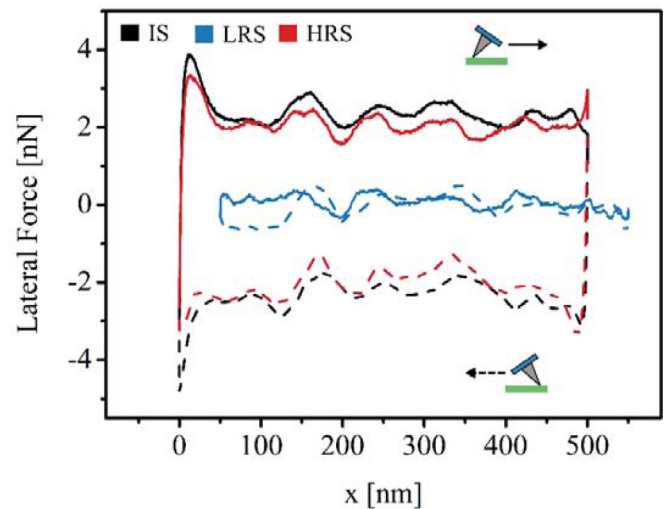ate, and thus must be caused by spatial heterogeneities in the specimen. The most likely explanation comes from the gradients in the local sample surface height dh/dx which contribute additively to the measured lateral force [23].

In order to confirm the robustness of the effect of the resistive state on friction forces, the above experiment was repeated for three different regions of interest on the specimen (Fig. 3). The average friction force for each $500 \times 500\,nm^2$ region of interest and resistive state was calculated by shifting the maps to align the topography, subtracting the forward and backward lateral forces, dividing by two, and averaging over the entire map. Despite a clear dependence of the initial friction on location, the friction for all regions is clearly reduced upon switching from the insulating IS to the conducting LRS and increases on switching back to the HRS. However, it is found that the friction force of the IS is not fully recovered on switching back from the LRS to the HRS. This observation is consistent with previous studies [19] where resistance fatigue was observed when switching a manganite thin film back and forth between its resistive states, particularly after the first switching cycle. Specifically, the difference between the resistances of the two states decreased with switching cycle number. Furthermore, Krisponeit *et al.* reported local variations in the threshold voltage and the magnitude of the resistance change on switching [19] as well as in the time stability of the LRS [20]. It is possible that the variations from region to region in the initial values of the friction and in the magnitude of the friction force change on switching may have the same origins as the local resistance variations. Whether the causes of resistance and friction variations are local variations in composition, surface charge density, thickness of the
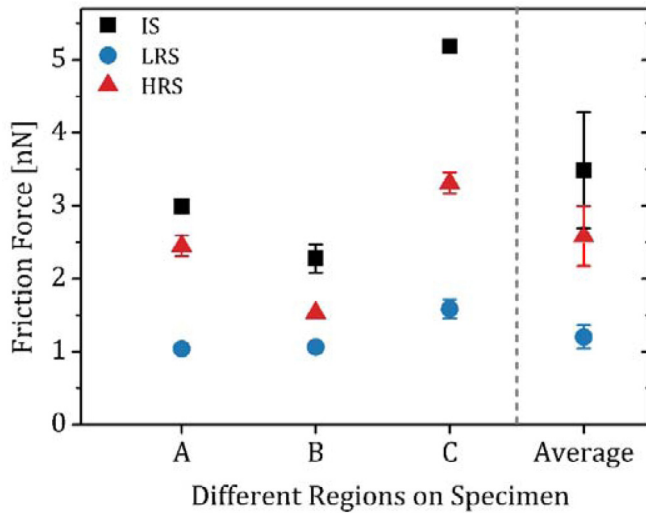
FIG. 3. Friction of the insulating state (IS and HRS) is consistently higher than of the metallic state (LRS) in three different regions A, B, and C of the $La_{0.55}Ca_{0.45}MnO_3$ film. The left-hand portion of the plot shows average values (symbols) and ranges (bars) for friction of each resistive state in the three regions. The means and standard deviation of the position-averaged values of the friction for each resistive state are shown in the right-hand portion of the plot.

FIG. 4. Friction force vs temperature for the $La_{0.55}Ca_{0.45}MnO_3$ film measured with a silicon (blue triangles) and a Pt-coated silicon tip (red circles). The dashed line shows a thermolubricity model fit to the silicon-tip data with an activation energy of 0.2 eV.

oxygen-deficient surface or dead layer [24,25], or some other effect is not yet clear.

The dependence of friction force on normal force in the initial resistive state has been studied by acquiring a series of friction loop maps for different normal forces (see Supplemental Material [17]). The friction force increases roughly linearly with applied normal force, with a positive intercept (see Supplemental Material [17]), in agreement with previous studies [26]. Even in the absence of an applied normal force ($F_N = 0$), the attractive adhesion force between the tip and specimen leads to nonzero friction forces. The increase of the friction force with normal force primarily reflects the increase in contact area. The well-behaved dependence of the friction force on the normal force (see Supplemental Material [17]) supports the robustness of the friction measurements as well as the fact that the variations observed in the friction force values in Figs. 2 and 3 are indeed the result of spatial heterogeneities.

In order to further investigate correlations between the near-surface properties and friction of the LCMO film, the friction force near the metal-to-insulator transition at 245 K was measured (Fig. 4). FFM maps were performed with the same methodology as above from an IS sample for temperatures between 110 and 300 K using both silicon- and Pt-coated silicon cantilevers. Measurements were performed at room temperature at the beginning and at the end of the temperature series to confirm that there had been no irreversible changes in the specimen or the AFM tip. The friction force measured with the Si tip decreases continuously with increasing temperature, while the friction force measured with the Pt-coated tip remains constant within the noise. Neither measurement series shows any effect of the metal-to-insulator transition on the friction.
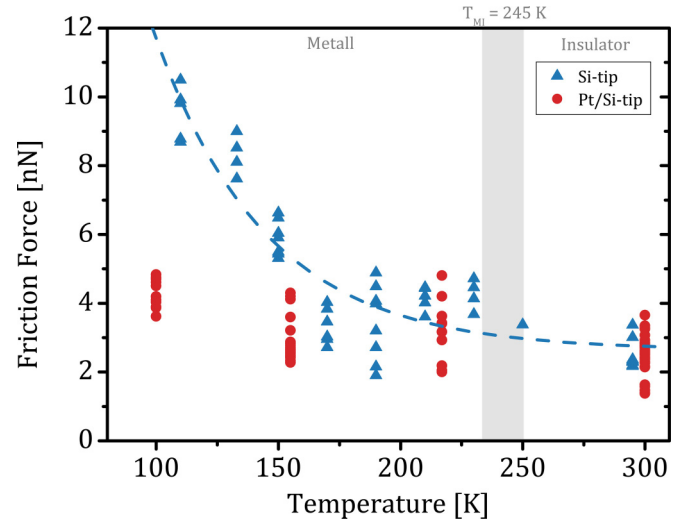
Changing the electronic properties by resistive switching causes a clear change in friction, while changing the electronic properties by a temperature-driven metal-to-insulator transition has no effect. The likely explanation for this is the approximately 1-nm-thick high-resistivity surface dead layer [24,25]. It is often argued that the surface dead layer is changed during resistive switching and may undergo a layer-by-layer electronic structural transformation [27] and/or exchange oxygen vacancies with the underlying film by electrochemical migration [15,18]. Both mechanisms are expected to produce changes in the near-surface structure and electronic properties. In contrast, the surface dead layer remains intact through the metal-to-insulator transition and is sufficiently thick to shield any contributions from the underlying film material. This temperature-dependent behavior is in excellent agreement with the so-called thermolubric effect [8,26], which attributes the widely observed thermally activated friction at cryogenic temperatures to adhesion hysteresis from making and breaking contacts between hard materials during sliding. A fit to the friction forces measured with a Si tip give an activation energy of 0.2 eV, which is within the range of those reported in the literature [26]. As observed in previous studies, thermolubricity is not observed for the Pt-coated tip, presumably due to the relatively easy deformation of the Pt surface, which leads to smearing in the interface rather than to making and breaking of adhesive contacts [8,26]. Thus, contact dynamics appear to entirely control the temperature dependence of the friction response in this case, while the metal-to-insulator transition in the buried film is not detected. It is conceivable that contributions from the transition in the underlying material might be detected more strongly for larger normal forces [8,28].

Contact sliding of two surfaces against each other causes a variety of different electronic interactions, including Ohmic losses and generation of electronic excitations [2,29]. However, theoretical estimates of the magnitudes of these effects

yield values no more than $F/v = 10^{-8}\,\mathrm{Ns/m}$, where F is the excess friction force due to the change in resistive state and v the scanning velocity [2]. Excess friction forces have been reported frequently in the literature and have been attributed to a variety of effects, including additional charge carriers [2,4], the superconducting transition [1,5,6,8] (the Cooper pairs in the superconducting state are assumed to be too tightly bound to be excited by friction [5]), and metal-to-insulator transitions [3,7]. However, the magnitude of the electronic effect observed for experimental contact friction measurements is many orders of magnitude larger than predicted by theory [29]. Even if one considers stick-slip motion of the tip, which would lead to intermittent substantially higher sliding speeds [30], theoretical predictions of electronic effects and slip velocities cannot explain the observed excess friction force. Only in cases such as noncontact dissipation measurements [5] and dissipation during adsorbate sliding [1,31] does the measured contribution show qualitative agreement with theory.

The disagreement between theory and contact friction experiments has largely been reconciled in the literature by considering the electrostatic forces that are generated between the two contacting materials as a result of contact electrification or tribo-electrification. These forces are in addition to any applied forces and will change the contact area between the two bodies. Particularly in oxides and other insulating materials, it has often been proposed that electrostatic forces from surface and other trapped charges may overwhelm other effects [2–4,6,10]. For example, Qi et al. [2] were able to obtain quantitative agreement with their experimental excess friction, which was on the order of $10^{-5}\,\mathrm{Ns/m}$, by accounting for the electrostatic forces from trapped charges in the surface oxide layer. Altfeder and Krim [6] found even larger excess dissipation levels in the range of 10^{-2}–$10^{-3}\,\mathrm{Ns/m}$ between the normal and superconducting phase of YBCO and attributed it to contact electrification and electrostatic effects in the oxygen-depleted surface layer of the normal phase. Kim et al. [3] also employed this argument to explain the large excess friction observed during pressure- and temperature-induced transformation of VO_2 from the insulating to metallic phase. Specifically, they attributed the excess friction to trapped charges in the surface V_2O_5 dielectric layer on the metallic VO_2 domains, leading to higher Coulomb attraction between the tip and sample. Finally, although preferring an explanation based on electron-phonon coupling, a recent study of the friction at the superconducting transition temperature of Pb also cannot rule out contributions from electrostatic forces [8].

In our studies of resistively switched friction, not only the magnitude of the excess friction due to changing the resistivity ($F/v = 10^{-3}$–$10^{-2}\,\mathrm{Ns/m}$) but even the direction of the friction change contradicts most existing theories for electronic excitations. We observe a clear reduction in friction on switching from the insulating to the conducting state. Thus, it seems highly unlikely that the friction changes observed here have their origins in electronic excitations. Instead, possible contributions from electrostatic forces to LCMO friction were tested by measuring the effect of an external voltage on adhesion for both the IS/HRS and LRS (Fig. 5). Force-distance measurements were performed at fixed locations on the film in both the HRS and LRS to obtain the adhesion (pull-off)
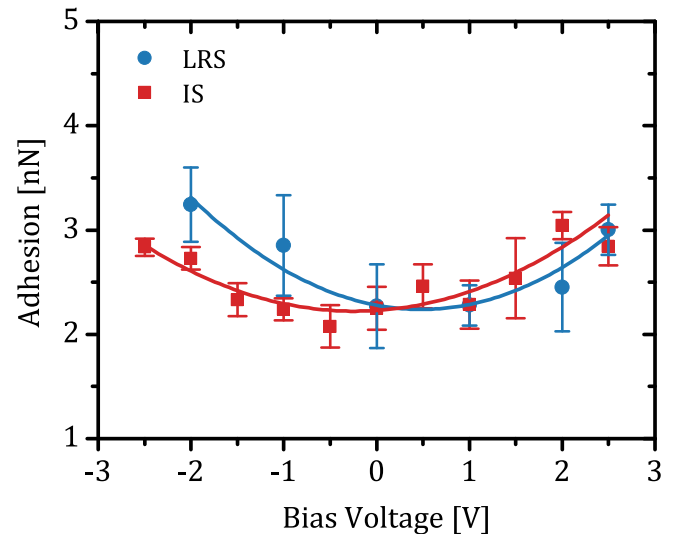

FIG. 5. Adhesion between a Pt-coated Si tip and a $La_{0.55}Ca_{0.45}MnO_3$ film as a function of the applied voltage for the insulating (IS) and conductive states (LRS) as determined from the pull-off force from five individual force-distance curves per voltage with their standard deviation as error. Solid lines are best fits to the data, including effects of capacitive forces and changes in contact area (see Supplemental Material [17]).

force as a function of the voltage applied between the LCMO film and a Pt-coated AFM tip. The applied voltage was kept below the threshold voltage to avoid unintentionally resistively switching the film. Pull-off occurs during tip retraction when the cantilever stiffness first exceeds the gradient in the tip-specimen interaction force. For the relatively compliant cantilever used here, pull-off occurs close to the point of maximum attractive force between the tip and specimen. Any changes in pull-off force with applied voltage are due to electrostatic forces between the Pt-coated Si tip and the specimen and the resultant increase in the contact area between the tip and specimen. Note that the tip used for this study was different from those used to measure the lateral friction force during resistive switching (Figs. 1 –3) so that the magnitude of the forces will generally not be directly comparable.

The adhesive force is found to be similar for the two resistive states and increases slightly with applied voltage (Fig. 5). The data have been fit with a simple model based on a Hertz contact and parallel-plate capacitance between the tip and specimen (see Supplemental Material [17]). The material parameters needed to fit the model fall within the range of parameters found in similar materials in the literature [32–34]. The roughly 50% increase in the adhesion force at the maximum applied voltage results from a 28% increase in the contact area and is split with a ratio of 1:8 between electrostatic forces and nonelectrostatic adhesive forces. The fact that the minimum adhesive forces are comparable in the two resistive states indicates that the elastic constants [35] and the effective tip-specimen capacitances are not significantly different. The shift of the voltage at the minimum by around 0.7 V between the two resistive states indicates a change in either the specimen work function and/or a shift in the density of near-surface trapped charges, such as from extrinsic inter-

face charges at the buried interface between the dead layer and the film.

The electrostatic forces are expected to also affect friction by increasing the normal force, which increases the contact area. Ignoring possible lateral electrostatic forces [2] for the moment, accounting for the observed effect of resistive switching on friction would require that the contact area between the tip and the HRS be around three times larger than to the LRS. Under the friction measurement conditions used here, where the specimen is electrically connected only through the tip, the electrostatic forces come from the contact potential difference between the tip and specimen and from any trapped charges or charges generated by tribo-electrification (which may be quite different from those generated by contact electrification [36]). However, since spontaneous resistive switching was not observed during the friction measurements, the maximum electric potential generated during friction must be less than the threshold voltage for switching, leading to a maximum change in contact area of 28%. We therefore believe we can rule out electrostatic forces as the dominant cause of the effect of resistive switching on the LCMO friction.

Having ruled out electronic excitations, electrostatic interactions, and changes in contact area (also due to changes in elastic properties [35]) as possible causes for the large and reversible change in friction due to resistive switching, we are left with dissipation by electron-phonon excitations as a possibility. Most of the systems where friction has been observed to change with the electronic state also involve changes in the phonon behavior. For example, the structural phase transformation in VO_2 and the superconducting transition involve changes in the phonon density of states as well as in the electron-phonon coupling. Also, for $La_{0.55}Ca_{0.45}MnO_3$ the phonon density of states changes quite strongly at the metal-to-insulator transition due to the formation of Jahn-Teller excitations. Assuming that sliding occurs by the generation and propagation of stick-slip excitations in the contact interface, the friction force will then be determined by the generation rate of slip pulse excitations and their lifetimes [9,37]. In fact, a model for the direct coupling of the coherent interface slip pulses that occur in the contact interface during sliding friction to phonons [38,39] shows that the phonon lifetime τ_{ph} determines the rate at which the energy of the slip pulses is spread and dissipated in the material. This leads to a friction force that is proportional to the phonon relaxation rate $F/v \propto 1/\tau_{ph}$ but also contains a nonlinear $\ln(v)$ dependence on the tip sliding velocity through the generation rate of slip pulse excitations [9,37]. Phonon relaxation rates can be estimated around the metal-to-insulator transition from thermal conductivity measurements, since the phonon contribution is expected to dominate over electron and magnon contributions. Changes in thermal conductivity and phonon lifetimes with temperature in various manganites are known to scale with static MnO_6 distortions [40]. For example, phonon scattering rates are estimated to decrease by a factor of 2.7 between the insulating phase (300 K) and the metallic phase (50 K) of $La_{0.7}Ca_{0.3}MnO_3$ [40], suggesting that the friction should decrease by the same factor. Assuming the MnO_6 distortions are similar in the equilibrium low-temperature metallic phase and the metastable resistively switched LRS phase, the phonon lifetime model provides an excellent explanation for both the sign and magnitude of the friction change observed here. Since distortion of the MnO_6 octahedra results from the interplay of lattice, charge, and spin degrees of freedom, strongly correlated materials such as the manganites offer promising systems for controlling friction.

IV. CONCLUSIONS

In conclusion, we have demonstrated control of nanoscale friction by resistively switching a manganite film using an electric field. A reproducible and reversible change in friction force is observed on changing between high and low resistance states. Contributions from pure electronic excitations, electrostatic interactions, and changes in contact area have been ruled out as the cause of the friction change. However, direct coupling of coherent slip pulse excitations in the interface to phonons in the surrounding material, which have different lifetimes in the metal and insulator phases, does provide a good explanation for the observations. Thus materials with strong electron-phonon or spin-phonon coupling are promising candidates for controlling friction by external fields [11]. Facile switching of friction forces would offer new control concepts for self-propelled directed motion as well as energy dissipation minimization at contact interfaces.

[1] A. Dayo, W. Alnasrallah, and J. Krim, Phys. Rev. Lett. **80**, 1690 (1998).

[2] Y. Qi, J. Y. Park, B. L. M. Hendriksen, D. F. Ogletree, and M. Salmeron, Phys. Rev. B **77**, 184105 (2008).

[3] J. H. Kim, D. Fu, S. Kwon, K. Liu, J. Wu, and J. Y. Park, Adv. Mater. Interfaces **3**, 1500388 (2016).

[4] J. Y. Park, D. F. Ogletree, P. A. Thiel, and M. Salmeron, Science **313**, 186 (2006).

[5] M. Kisiel, E. Gnecco, U. Gysin, L. Marot, S. Rast, and E. Meyer, Nat. Mater. **10**, 119 (2011).

[6] I. Altfeder and J. Krim, J. Appl. Phys. **111**, 094916 (2012).

[7] D. Singh, P. Mittal, N. N. Gosvami, and V. Balakrishnan, Adv. Eng. Mat. **21**, 1900616 (2019).

[8] W. Wang, D. Dietzel, and A. Schirmeisen, Sci. Adv. **6**, eaay0165 (2020).

[9] N. A. Weber, H. Schmidt, T. Sievert, C. Jooss, F. Güthoff, V. Moshneaga, K. Samwer, M. Krüger, and C. A. Volkert, arXiv:2009.12137.

[10] B. N. Persson and E. Tosatti, Surf. Sci. **411**, L855 (1998).

[11] J. Krim, Front. Mech. Eng. **5**, 22 (2019).

[12] J. M. D. Coey, M. Viret, and S. von Molnar, Adv. Phys. **48**, 167 (1999).

[13] P. Schiffer, A. P. Ramirez, W. Bao, and S. W. Cheong, Phys. Rev. Lett. **75**, 3336 (1995).

[14] R. von Helmolt, J. Wecker, B. Holzapfel, L. Schultz, and K. Samwer, Phys. Rev. Lett. **71**, 2331 (1993).

[15] A. Sawa, Mater. Today **11**, 28 (2008).

[16] V. Moshnyaga, I. Khoroshun, A. Sidorenko, P. Petrenko, A. Weidinger, M. Zeitler, B. Rauschenbach, R. Tidecks, and K. Samwer, Appl. Phys. Lett. **74**, 2842 (1999).

[17] See Supplemental Material at http://link.aps.org/supplemental/10.1103/PhysRevMaterials.4.113610 for a θ-2θ x-ray diffraction spectrum and four-point resistance measurement versus temperature of the $La_{0.55}Ca_{0.45}MnO_3$ film, for current maps in the different resistive states, for a plot of friction force versus normal force, and for a model of the effect of voltage on adhesion forces.

[18] R. Yang, X. M. Li, W. D. Yu, X. D. Gao, D. S. Shang, X. J. Liu, X. Cao, Q. Wang, and L. D. Chen, Appl. Phys. Lett. **95**, 072105 (2009).

[19] J. O. Krisponeit, C. Kalkert, B. Damaschke, V. Moshnyaga, and K. Samwer, Phys. Rev. B **82**, 144440 (2010).

[20] J. O. Krisponeit, C. Kalkert, B. Damaschke, V. Moshnyaga, and K. Samwer, Phys. Rev. B **87**, 121103(R) (2013).

[21] *Nanotribology and Nanomechanics II*, edited by B. Bhushan (Springer, Berlin, 2011).

[22] E. Gnecco, R. Bennewitz, T. Gyalog, and E. Meyer, J. Phys.: Condens. Matter **13**, R619 (2001).

[23] S. Grafstrom, M. Neitzert, T. Hagen, J. Ackermann, R. Neumann, O. Probst, and M. Wortge, J. Nanotechnol. **4**, 143 (1993).

[24] M. J. Calderón, L. Brey, and F. Guinea, Phys. Rev. B **60**, 6698 (1999).

[25] S. Merten, V. Bruchmann-Bamberg, B. Damaschke, K. Samwer, and V. Moshnyaga, Phys. Rev. Mater. **3**, 060401 (2019).

[26] I. Barel, M. Urbakh, L. Jansen, and A. Schirmeisen, Tribol. Lett. **39**, 311 (2010).

[27] J. O. Krisponeit, B. Damaschke, V. Moshnyaga, and K. Samwer, Phys. Rev. Lett. **122**, 136801 (2019).

[28] V. Pfahl, M. K. Phani, M. Büchsenschütz-Göbeler, A. Kumar, V. Moshnyaga, W. Arnold, and K. Samwer, Appl. Phys. Lett. **110**, 053102 (2017).

[29] B. N. J. Persson, *Sliding Friction* (Springer, Berlin, 2000).

[30] J. Krim, P. Yu, and R. P. Behringer, Pure Appl. Geophys. **168**, 2259 (2011).

[31] M. Highland and J. Krim, Phys. Rev. Lett. **96**, 226107 (2006).

[32] O. Cherniavskaya, L. Chen, V. Weng, L. Yuditsky, and L. E. Brus, J. Phys. Chem. B **107**, 1525 (2003).

[33] F. Johann, A. Hoffmann, and E. Soergel, Phys. Rev. B **81**, 094109 (2010).

[34] S. Hong, S. M. Nakhmanson, and D. D. Fong, Rep. Prog. Phys. **79**, 076501 (2016).

[35] J. H. So, J. R. Gladden, Y. F. Hu, J. D. Maynard, and Q. Li, Phys. Rev. Lett. **90**, 036103 (2003).

[36] R. Xu, S. Ye, K. Xu, L. Lei, S. Hussain, Z. Zheng, F. Pang, S. Xing, X. Liu, W. Ji, and Z. Cheng, Nanotechnology **29**, 355701 (2018).

[37] Z. Wei, Z. Duan, Y. Kann, Y. Zhang, and Y. Chen, J. Appl. Phys. **127**, 015105 (2020).

[38] M. Cieplak, E. D. Smith, and M. O. Robbins, Science **265**, 1209 (1994).

[39] E. D. Smith, M. O. Robbins, and M. Cieplak, Phys. Rev. B **54**, 8252 (1996).

[40] J. L. Cohn, J. J. Neumeier, C. P. Popoviciu, K. J. McClellan, and Th. Leventouri, Phys. Rev. B **56**, R8495 (1997).